

## Measurement of Excitation Spectra in the $^{12}\text{C}(p, d)$ Reaction near the $\eta'$ Emission Threshold

Y. K. Tanaka,<sup>1,\*</sup> K. Itahashi,<sup>2,†</sup> H. Fujioka,<sup>3,‡</sup> Y. Ayyad,<sup>4</sup> J. Benlliure,<sup>5</sup> K.-T. Brinkmann,<sup>6</sup> S. Friedrich,<sup>6</sup> H. Geissel,<sup>6,7</sup> J. Gellanki,<sup>8</sup> C. Guo,<sup>9</sup> E. Gutz,<sup>6</sup> E. Haettner,<sup>7</sup> M. N. Harakeh,<sup>8</sup> R. S. Hayano,<sup>1</sup> Y. Higashi,<sup>10</sup> S. Hirenzaki,<sup>10</sup> C. Hornung,<sup>6</sup> Y. Igarashi,<sup>11</sup> N. Ikeno,<sup>12</sup> M. Iwasaki,<sup>2</sup> D. Jido,<sup>13</sup> N. Kalantar-Nayestanaki,<sup>8</sup> R. Kanungo,<sup>14</sup> R. Knöbel,<sup>6,7</sup> N. Kurz,<sup>7</sup> V. Metag,<sup>6</sup> I. Mukha,<sup>7</sup> T. Nagae,<sup>3</sup> H. Nagahiro,<sup>10</sup> M. Nanova,<sup>6</sup> T. Nishi,<sup>2</sup> H. J. Ong,<sup>4</sup> S. Pietri,<sup>7</sup> A. Prochazka,<sup>7</sup> C. Rappold,<sup>7</sup> M. P. Reiter,<sup>7</sup> J. L. Rodríguez-Sánchez,<sup>5</sup> C. Scheidenberger,<sup>6,7</sup> H. Simon,<sup>7</sup> B. Sitar,<sup>15</sup> P. Strmen,<sup>15</sup> B. Sun,<sup>9</sup> K. Suzuki,<sup>16</sup> I. Szarka,<sup>15</sup> M. Takechi,<sup>17</sup> I. Tanihata,<sup>4,9</sup> S. Terashima,<sup>9</sup> Y. N. Watanabe,<sup>1</sup> H. Weick,<sup>7</sup> E. Widmann,<sup>16</sup> J. S. Winfield,<sup>7</sup> X. Xu,<sup>6,7</sup> H. Yamakami,<sup>3</sup> and J. Zhao<sup>9</sup>

( $\eta$ -PRiME/Super-FRS Collaboration)

<sup>1</sup>The University of Tokyo, 7-3-1 Hongo, Bunkyo, 113-0033 Tokyo, Japan

<sup>2</sup>Nishina Center for Accelerator-Based Science, RIKEN, 2-1 Hirosawa, Wako, 351-0198 Saitama, Japan

<sup>3</sup>Kyoto University, Kitashirakawa-Oiwakecho, Sakyo-ku, 606-8502 Kyoto, Japan

<sup>4</sup>RCNP, Osaka University, 10-1 Mihogaoka, Ibaraki, 567-0047 Osaka, Japan

<sup>5</sup>Universidade de Santiago de Compostela, 15782 Santiago de Compostela, Spain

<sup>6</sup>Universität Giessen, Heinrich-Buff-Ring 16, 35392 Giessen, Germany

<sup>7</sup>GSI Helmholtzzentrum für Schwerionenforschung GmbH, Planckstraße 1, 64291 Darmstadt, Germany

<sup>8</sup>KVI-CART, University of Groningen, Zernikelaan 25, 9747 AA Groningen, The Netherlands

<sup>9</sup>Beihang University, Xueyuan Road 37, Haidian District, 100191 Beijing, China

<sup>10</sup>Nara Women's University, Kita-Uoya Nishi-Machi, 630-8506 Nara, Japan

<sup>11</sup>KEK, 1-1 Oho, Tsukuba, 305-0801 Ibaraki, Japan

<sup>12</sup>Tottori University, 4-101 Koyamacho-minami, 680-8551 Tottori, Japan

<sup>13</sup>Tokyo Metropolitan University, 1-1 Minami-Osawa, Hachioji, 192-0397 Tokyo, Japan

<sup>14</sup>Saint Mary's University, 923 Robie Street, Halifax, Nova Scotia B3H 3C3, Canada

<sup>15</sup>Comenius University Bratislava, Mlynská dolina, 842 48 Bratislava, Slovakia

<sup>16</sup>Stefan-Meyer-Institut für subatomare Physik, Boltzmannsgasse 3, 1090 Vienna, Austria

<sup>17</sup>Niigata University, 8050 Ikarashi 2-no-cho, Nishi-ku, 950-2181 Niigata, Japan

(Received 11 May 2016; revised manuscript received 25 August 2016; published 8 November 2016)

Excitation spectra of  $^{11}\text{C}$  are measured in the  $^{12}\text{C}(p, d)$  reaction near the  $\eta'$  emission threshold. A proton beam extracted from the synchrotron SIS-18 at GSI with an incident energy of 2.5 GeV impinges on a carbon target. The momenta of deuterons emitted at  $0^\circ$  are precisely measured with the fragment separator (FRS) operated as a spectrometer. In contrast to theoretical predictions on the possible existence of deeply bound  $\eta'$ -mesic states in carbon nuclei, no distinct structures are observed associated with the formation of bound states. The spectra are analyzed to set stringent constraints on the formation cross section and on the hitherto barely known  $\eta'$ -nucleus interaction.

DOI: 10.1103/PhysRevLett.117.202501

The mass of the  $\eta'$  meson is exceptionally large (958 MeV/ $c^2$ ) compared with other mesons in the same pseudoscalar multiplet. This large mass is known as the “U(1) problem” raised by Weinberg [1]. Since the origin of the exceptionally large mass is attributed to the effect of the  $U_A(1)$  anomaly in QCD (quantum chromodynamics) under the presence of the spontaneous breaking of chiral symmetry, it is natural to expect a weakening of such an anomaly effect in a nuclear medium, where chiral symmetry may partially be restored [2,3]. This suppression of the anomaly effect would lead to a large mass reduction in a nuclear medium [4]. Recent model calculations have predicted a 4%–15% mass reduction at normal nuclear

density [5–8]. Thus, the observation of such a modification would provide novel insights into strongly interacting many-body systems and the QCD vacuum.

A mesic atom or nucleus, which is a bound state of a meson and a nucleus, will offer a testing ground for the investigation of in-medium meson properties which can be different from those in the QCD vacuum due to the partial restoration of chiral symmetry [2,3]. For example, deeply bound pionic atoms in nuclei, in which a modification of the isovector part of the  $s$ -wave pion-nucleus potential manifests itself, are very well-established systems [9,10]. Distinct peak structures corresponding to pionic states with different configurations, especially pions in the atomic 1s

state, can be identified in the missing-mass spectrum of the ( $d$ ,  $^3\text{He}$ ) reaction [11]. In contrast to invariant-mass spectroscopy of hadrons decaying into multiparticle final states in a nuclear medium, missing-mass spectroscopy is an alternative approach providing experimental access to in-medium meson properties.

In addition, a quantum many-body system, such as an atomic nucleus, exhibits various phenomena which cannot be observed in a two-body system. The strong interaction is indeed “strong” in that a typical binding energy of a particle relative to its rest energy is large, in contrast to the electromagnetic interaction, which binds an electron and an atomic nucleus. Hence, the subthreshold behavior of two-body interactions is of importance in building up a many-body system. This may also be the case for the  $\eta'$ -nucleon interaction.

The mass reduction of the  $\eta'$  meson leads to an attractive interaction between an  $\eta'$  meson and a nucleus. Hence, an experimental observation of  $\eta'$ -nucleus bound states may provide a direct clue for deducing the  $\eta'$  mass at normal nuclear density. It should be noted that a clear distinction of neighboring levels in a spectrum requires a rather narrow absorption width. Numerical results of an  $\eta'$ -nucleus optical potential based on a chiral unitary model show that the depth of the imaginary part of the potential (half absorption width) is much smaller than that of the real part (mass reduction), regardless of the strength of the two-body  $\eta'N$  interaction [12].

Experimental information on low-energy  $\eta'$ -nucleus interaction is very limited. A recent measurement of  $\eta'$  photoproduction and the emission from nuclei at CBELSA/TAPS was utilized to evaluate the  $\eta'$ -nucleus optical potential for the first time [13]. The absorption width, for the average  $\eta'$  momentum of 1050 MeV/ $c$ , was deduced to be 15–25 MeV at normal nuclear density, from a measurement of the transparency ratio of  $\eta'$  mesons propagating in various nuclear targets [14]. Furthermore, the excitation function and the momentum distribution of  $\eta'$  mesons, produced and emitted from  $^{12}\text{C}$ , were compared with a model calculation with the real part of the potential as a free parameter leading to a potential depth of  $-37 \pm 10(\text{stat}) \pm 10(\text{syst})$  MeV [13]. In contrast, a small  $\eta'N$  scattering length with a real part consistent with zero was obtained from the excitation function of the  $pp \rightarrow pp\eta'$  reaction very close to the threshold [15].

As can be inferred from the  $\eta$ -nucleon and  $\eta$ -nucleus interactions, which have been investigated in a variety of reactions [16,17], it is far from straightforward to extrapolate the on-shell scattering amplitude to the subthreshold region, pointing to the importance of meson-nucleus bound systems, serving as a unique probe of subthreshold behavior.

A direct measurement of the in-medium mass reduction was proposed by spectroscopy of  $\eta'$  bound states in a nucleus by measuring an excitation spectrum of  $^{11}\text{C}$  in the  $^{12}\text{C}(p, d)$  reaction near the  $\eta'$  emission threshold [18]. Theoretical calculations indicated the possible existence of

such bound states. One based on the Nambu–Jona-Lasinio (NJL) model predicted a sufficiently attractive potential of  $-150$  MeV [5,6] to accommodate  $\eta'$  in a carbon nucleus, provided that the absorption is not too strong. Considerations on the momentum transfer and the differential cross section of the elementary  $n(p, d)\eta'$  reaction led to a preferable incident proton energy of 2.5 GeV.

As discussed in Ref. [18], excitation energy spectra were predicted for different assumed  $\eta'$ -nucleus interactions expressed by attractive real and absorptive imaginary potential depths ( $V_0, iW_0$ ) MeV at the nuclear center. The predicted spectra demonstrated the experimental sensitivity for the bound states and the advantage of an unbiased spectral analysis in an inclusive measurement that surpasses the disadvantages of a small signal-to-noise ratio mainly arising from large cross sections of multiple pion production in the reaction. Thus, we aimed at a region where attraction is relatively strong and absorption is weak by achieving extremely good statistics of  $\leq 1\%$  relative errors and a moderate resolution of  $\leq 10$  MeV over the spectral region of interest.

The  $^{11}\text{C}$  excitation spectra were measured near the  $\eta'$  emission threshold using the  $^{12}\text{C}(p, d)$  reaction at zero degrees. We employed a proton beam with the energy of  $2499.1 \pm 2.0$  MeV extracted from the synchrotron SIS-18 at GSI, Darmstadt, Germany, impinging on a carbon target of natural isotopic composition with a thickness of  $4.115 \pm 0.001$  g/cm $^2$ . The beam intensity was  $\sim 10^{10}$ /s and the spill length and the cycle were 4 and 7 s, respectively. The intensity was directly measured with an uncertainty of 5.5% by inserting a detector, SEETRAM [19], in the beam near the target. The typical horizontal beam spot size was 1 mm.

The emitted deuterons had a momentum of 2814.4 MeV/ $c$  at the  $\eta'$  production threshold after energy loss in the target and were momentum analyzed by the FRS [20] used as a spectrometer with a specially developed ion optical setting. The central focal plane ( $F2$ ) was momentum-achromatic and the final focal plane ( $F4$ ) was dispersive with a designed momentum resolving power of  $3.8 \times 10^3$ . The  $F4$  dispersion was measured to be 3.51 cm/%. The deuteron tracks were measured by two sets of MWDCs (multiwire drift chambers) separately installed at a distance of about one meter near  $F4$ , as depicted in Fig. 1.

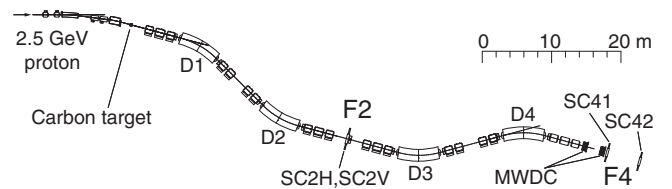


FIG. 1. A schematic view of the FRS used as a spectrometer and detectors used in the present analysis. A 2.5 GeV proton beam impinged on a carbon target. Deuterons emitted in the  $^{12}\text{C}(p, d)$  reaction were momentum analyzed at  $F4$  and the tracks were measured by MWDCs. Sets of 5 mm-thick plastic scintillation counters (SC2H, SC2V, and SC41) and a 20 mm-thick one (SC42) were installed at  $F2$  and  $F4$  for a TOF measurement.

Four sets of plastic scintillation counters installed at  $F2$  and  $F4$  identified the particles by measuring the time of flight (TOF) for signal deuterons ( $\sim 150$  ns) and for background protons ( $\sim 132$  ns). Count rates at  $F4$  during the spill extraction were  $\sim 250$  kHz for protons and  $\sim 1$  kHz for deuterons. 99.5% of the protons were rejected in the TOF-based triggers, while  $\sim 100\%$  of the deuterons were selected. The data acquisition live rate ranged between 30% and 40%, and the recorded trigger rate varied around 1 kHz during the spill extraction. After further selection based on the waveform analyses of photomultiplier tube signals of the scintillation counters rejecting multiple hits, we achieved  $\leq 4\%$  deuteron overkill in the analysis with a very small ( $\sim 2 \times 10^{-4}$ ) proton contamination fraction of the deuteron identified events.

During the measurement, we accumulated data to cover a wider energy region spanning between  $-91$  and  $+34$  MeV around the  $\eta'$  emission threshold by scaling all FRS magnets with seven factors between 0.980 and 1.020. An excitation energy range of  $\sim 35$  MeV was covered in one setting by the central acceptance region, where one could safely rely on the momentum acceptance of the spectrometer. The momentum acceptance was determined by the code MOCADI [21] simulating the particle tracks based on the geometries of the magnets, the ion optical transport, the apertures of the beam pipes, effects of the materials, and the detector performances. The uncertainties in the acceptance estimation were taken into account in the subsequent analyses.

The central momenta of the seven settings were calibrated by using an elastic  $D(p, d)$  reaction on a deuterated polyethylene ( $CD_2$ ) target with a thickness of  $1.027 \pm 0.002$  g/cm<sup>2</sup> using a  $1621.6 \pm 0.8$  MeV proton beam. Nearly monoenergetic deuterons with a momentum of  $2828.0 \pm 1.0$  MeV/c were emitted forward within the solid angle of the FRS (horizontal,  $\pm 15$  mrad; vertical,  $\pm 20$  mrad). We also evaluated the ion optical aberrations from the measured correlations between positions and angles and adopted the corrections. The calibration data were taken every 8 h during the total 70.5 h of production measurement and confirmed the stability of the spectrometer system.

The momentum spectra for seven central-momentum settings were combined after the acceptance and optical aberration corrections by fitting the spectra in the overlap regions of neighboring settings. Note here that this procedure decreased the degrees of freedom of the data, which turned out to cause minor influences, as we discuss below.

Figure 2 (top panel) shows the measured excitation spectrum of the  $^{12}C(p, d)$  reaction near the  $\eta'$  emission threshold. The excitation energy  $E_{\text{ex}}$  relative to the threshold  $E_0 = 957.78$  MeV is shown by the bottom axis and the deuteron momentum by the top axis. The ordinate is the double differential cross section of the reaction at zero degrees which has an error of  $\pm 13\%$  in the absolute scale mainly as a result of the uncertainties in the incident beam intensities and

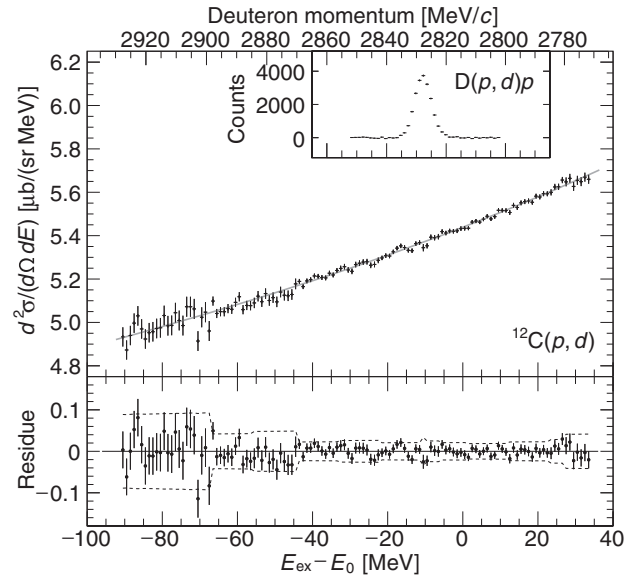


FIG. 2. (Top panel) Excitation spectrum of  $^{12}C$  measured in the  $^{12}C(p, d)$  reaction at a proton energy of 2.5 GeV. The abscissa is the excitation energy  $E_{\text{ex}}$  referring to the  $\eta'$  emission threshold  $E_0 = 957.78$  MeV. The overlaid gray solid curve displays a fit of the spectrum with a third-order polynomial. The upper horizontal axis shows the deuteron momentum scale. (Inset) Deuteron momentum spectrum measured in the elastic  $D(p, d)p$  reaction using a 1.6 GeV proton beam. (Bottom panel) Fit residues with envelopes of 2 standard deviations.

in the solid angle. The systematic error associated with the excitation energy is deduced to be 1.7 MeV, mainly owing to the uncertainties of the beam energies.

No distinct narrow structure has been observed in the excitation spectrum in spite of the extremely good statistical sensitivity at a level of better than 1%. The measured cross section steadily increases from 4.9 to  $5.7 \mu\text{b}/(\text{sr MeV})$  within the measured excitation energy region that ranges from  $-91$  to  $+34$  MeV and agrees within an order of magnitude with the simulated cross sections of the quasi-free processes  $pN \rightarrow dX$  ( $X = 2\pi, 3\pi, 4\pi, \omega$ ) [18], where  $N$  denotes a nucleon in a carbon nucleus. The measured spectrum has been fitted over the whole region by a third-order polynomial displayed as a solid gray curve where  $\chi^2$  and the number of degrees of freedom are 119 and 121, respectively. For positive excitation energies, the fit may include increasing contributions from quasifree  $\eta'$  production, estimated to reach the order of some 10 nb/(sr MeV) at  $E_{\text{ex}} - E_0 = 30$  MeV [22]. The fitting residues are shown in the bottom panel with envelopes of 2 standard deviations. No significant structure is observed. Note that the jumps in the envelope reflect the edges between two neighboring spectrometer settings.

The inset displays the measured momentum distribution of elastically scattered deuterons in a calibration measurement  $D(p, d)p$  with the  $CD_2$  target after subtracting the carbon contribution, demonstrating the symmetrical

response of the momentum measurement. The energy resolution during the production runs has been estimated by fitting the spectrum with a Gaussian function to yield  $\sigma_{\text{exp}} = 2.5 \pm 0.1$  MeV over the whole energy region after considering the energy losses in the targets and the momentum spreads of the incident beams.

Since no distinct structure has been observed in the spectrum, we have deduced upper limits of the formation cross section of  $\eta'$ -mesic nuclei as a function of the excitation energy  $E_{\text{ex}}$  and the width  $\Gamma$  (FWHM). We have assumed that the spectrum has two components, a smooth continuous part that is expressed by a third-order polynomial and a formation cross section of  $\eta'$ -mesic nuclei given by a Voigt function, i.e., a Lorentzian function with the width  $\Gamma$  folded by a Gaussian function with the width of  $\sigma_{\text{exp}}$ . The spectrum has been fitted by the sum of the two components within a region of  $\pm 35$  MeV around the Lorentzian center with the height of the Voigt function and four coefficients of the polynomial as free parameters. We have evaluated upper limits at the 95% confidence level, assuming the probability-density functions to be Gaussian, integrating them in the physical non-negative regions, and finding points where 95% of the probability-density-function areas have been covered by the regions beneath.

Repeating the above procedure by changing the Lorentzian positions and widths, we have obtained upper limits for the region encompassing  $-60 \text{ MeV} \leq E_{\text{ex}} - E_0 \leq +20 \text{ MeV}$  and  $\Gamma = 5, 10, 15$  MeV, as indicated by the solid curves in Fig. 3. The limits in the differential cross section  $d\sigma/d\Omega$  are indicated by the vertical axis on the left and those in the Lorentzian heights  $d^2\sigma/(d\Omega dE)$  by the three scales on the right side for each  $\Gamma$ . Typical systematic errors are indicated by the vertical

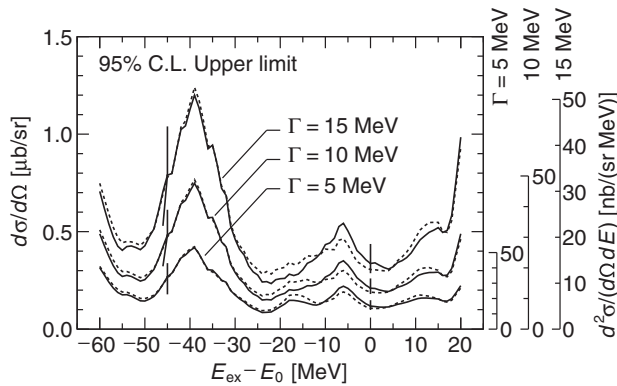


FIG. 3. Upper limits for the formation cross section of  $\eta'$ -mesic nuclei at the 95% confidence levels evaluated by two methods, namely, by fitting the combined spectrum (Fig. 2) shown by the solid lines and by simultaneously fitting the spectra for seven central-momentum settings (the dashed lines). The limits are presented as functions of the excitation energy  $E_{\text{ex}}$  for three tested natural widths:  $\Gamma = 5, 10, 15$  MeV. The scales to the right indicate the upper limits of the differential cross sections at the heights of the Lorentzian function for each tested natural width. Typical systematic errors are shown by the vertical

bars, which arise from the uncertainties in the beam intensity, the beam energy, the spectrometer acceptance, and the spectral resolution, and by moving the fitting boundaries by  $\pm 5$  MeV. We have set upper limits that are particularly rigid near the  $\eta'$  emission threshold:  $0.1\text{--}0.2 \mu\text{b}/\text{sr}$  for  $\Gamma = 5$  MeV,  $0.2\text{--}0.4 \mu\text{b}/\text{sr}$  for  $\Gamma = 10$  MeV, and  $0.3\text{--}0.6 \mu\text{b}/\text{sr}$  for  $\Gamma = 15$  MeV. The above analysis has been checked by a nearly identical procedure on the separate spectra for the seven spectrometer settings. Simultaneous fitting on each spectrum has yielded results shown by the dashed curves in Fig. 3, which are consistent with those in the analysis of the combined spectrum.

The resulting upper limits near the threshold of the peak height  $\sim 20$  nb/(sr MeV) exclude the existence of narrow peak structures with a height as great as  $40$  nb/(sr MeV) expected for potential parameters  $(V_0, W_0) = (-150, -10)$  MeV [22], which was predicted by a theoretical calculation based on the NJL model [6] and the absorption width suggested by the measured transparency ratio [14].

For further discussion of the constraints set on the  $\eta'$ -nucleus interaction, we have compared the combined spectrum with theoretical spectra described in Ref. [22] in a space of potential parameters  $(|V_0|, |W_0|)$ . For each potential-parameter combination of  $|V_0| = \{50, 100, 150, 200\}$  MeV  $\times$   $|W_0| = \{5, 10, 15, 20\}$  MeV and  $|V_0| = \{60, 80\}$  MeV  $\times$   $|W_0| = \{5, 10, 15\}$  MeV, the spectrum has been fitted in an energy region ranging from  $-40$  to  $30$  MeV by a sum of a third-order polynomial and a theoretical spectrum scaled by a scale parameter  $\mu$  and folded by a Gaussian function with the spectral resolution  $\sigma_{\text{exp}}$ . Wider ( $[-45, 35]$  MeV) and narrower ( $[-35, 25]$  MeV) fit regions have also been tested. In a similar way, upper limits of the scale parameter  $\mu_{95}$  have been evaluated at the 95% C.L. and are displayed on a potential-parameter plane in Fig. 4 after linear interpolation between

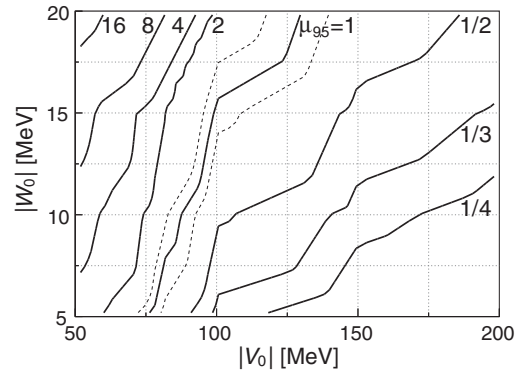


FIG. 4. A contour plot of  $\mu_{95}$  (the solid curves), upper limit of the scale parameter  $\mu$  at the 95% C.L., on a plane of real and imaginary potential parameters  $(|V_0|, |W_0|)$ . The limits have been evaluated for the potential-parameter combinations  $(V_0, W_0)$  in  $\{-50, -100, -150, -200\} \times \{-5, -10, -15, -20\}$  and  $\{-60, -80\} \times \{-5, -10, -15\}$  MeV and linearly interpolated in between. Dashed curves show a band of  $\mu_{95} = 1$  contour indicating the systematic errors. Regions for  $\mu_{95} \leq 1$  are excluded by the present analysis.

the calculated points. The dashed curves show  $\mu_{95} = 1$  in a band accounting for the estimated systematic errors.

Looking closely at Fig. 4, one finds that more stringent constraints (expressed by smaller  $\mu_{95}$ 's) are set for larger  $|V_0|$ 's and smaller  $|W_0|$ 's. Potential-parameter sets giving  $\mu_{95}$  smaller than 1 are excluded by the 95% C.L. within the present analysis. Note here that theoretical calculations are subject to an uncertainty [23] of a factor of 2 originating in the estimate of the cross section of the elementary process  $pn \rightarrow d\eta'$  of  $30 \mu\text{b/sr}$  [18], which has not yet been determined experimentally, and the experimental determination is of particular importance. Thus, the  $\mu_{95} = 1/2$  contour, for instance, corresponds to a 95% C.L. upper limit for the case that the absolute theoretical cross section was overestimated by a factor of  $1/\mu_{95} = 2$ .

In conclusion, we have conducted a high accuracy measurement of the excitation spectrum of the  $^{12}\text{C}(p, d)$  reaction near the  $\eta'$  emission threshold. We accomplished targeted statistical significance, spectral resolution, and overall accuracy in the measurement. No distinct structures are observed in the spectrum. Thus, a strongly attractive potential of  $V_0 \sim -150$  MeV predicted by the NJL model [6] is rejected for a relatively shallow imaginary potential of  $|W_0| \sim 10$  MeV [14]. The present experiment has only limited sensitivity for relatively weak attraction implied by the  $\eta'N$  scattering length [15] and suggested by the  $\eta'$  photoproduction experiments [13]. In the near future, we will extend the experimental sensitivity by constructing a detector system to efficiently select events originating from the formation of  $\eta'$ -mesic nuclei by tagging the decay particles in an experiment at GSI/FAIR. We will also consider the possibilities of using other reaction channels, such as  $(\pi, N)$ .

The authors acknowledge the GSI staffs for their support and the staffs of Institut für Kernphysik, Forschungszentrum Jülich for a test at COSY. We also thank Dr. M. Tabata for a specially developed aerogel. Y. K. T. acknowledges financial support from a Grant-in-Aid for JSPS Fellows (Grant No. 258155) and H. F. from Kyoto University Young Scholars Overseas Visit Program. This work is partly supported by MEXT Grants-in-Aid for Scientific Research on Innovative Areas (Grants No. JP24105705 and No. JP24105712), JSPS Grants-in-Aid for Scientific Research (S) (Grant No. JP23224008) and for Young Scientists (A) (Grant No. JP25707018), by the National Natural Science Foundation of China (Grant No. 11235002), and by the Bundesministerium für Bildung und Forschung.

\*Present address: GSI Helmholtzzentrum für Schwerionenforschung GmbH, Planckstraße 1, 64291 Darmstadt, Germany.

†itahashi@riken.jp

‡fujioka@scphys.kyoto-u.ac.jp

- [1] S. Weinberg, The U(1) problem, *Phys. Rev. D* **11**, 3583 (1975).
- [2] R. S. Hayano and T. Hatsuda, Hadron properties in the nuclear medium, *Rev. Mod. Phys.* **82**, 2949 (2010).
- [3] S. Leupold, V. Metag, and U. Mosel, Hadrons in strongly interacting matter, *Int. J. Mod. Phys. E* **19**, 147 (2010).
- [4] D. Jido, H. Nagahiro, and S. Hirenzaki, Nuclear bound state of  $\eta'$ (958) and partial restoration of chiral symmetry in the  $\eta'$  mass, *Phys. Rev. C* **85**, 032201(R) (2012).
- [5] P. Costa, M. C. Ruivo, C. A. de Sousa, and Yu. L. Kalinovsky, Analysis of  $U_A(1)$  symmetry breaking and restoration effects on the scalar-pseudoscalar meson spectrum, *Phys. Rev. D* **71**, 116002 (2005).
- [6] H. Nagahiro, M. Takizawa, and S. Hirenzaki,  $\eta$ - and  $\eta'$ -mesic nuclei and  $U_A(1)$  anomaly at finite density, *Phys. Rev. C* **74**, 045203 (2006).
- [7] S. D. Bass and A. W. Thomas,  $\eta$  bound states in nuclei: A probe of flavour-singlet dynamics, *Phys. Lett. B* **634**, 368 (2006).
- [8] S. Sakai and D. Jido, In-medium  $\eta'$  mass and  $\eta'N$  interaction based on chiral effective theory, *Phys. Rev. C* **88**, 064906 (2013).
- [9] K. Suzuki *et al.*, Precision Spectroscopy of Pionic  $1s$  States of Sn Nuclei and Evidence for Partial Restoration of Chiral Symmetry in the Nuclear Medium, *Phys. Rev. Lett.* **92**, 072302 (2004).
- [10] T. Yamazaki, S. Hirenzaki, R. S. Hayano, and H. Toki, Deeply bound pionic states in heavy nuclei, *Phys. Rep.* **514**, 1 (2012).
- [11] H. Gilg *et al.*, Deeply bound  $\pi^-$  states in  $^{207}\text{Pb}$  formed in the  $^{208}\text{Pb}(d, ^3\text{He})$  reaction. I. Experimental method and results, *Phys. Rev. C* **62**, 025201 (2000); K. Itahashi *et al.*, Deeply bound  $\pi^-$  states in  $^{207}\text{Pb}$  formed in the  $^{208}\text{Pb}(d, ^3\text{He})$  reaction. II. Deduced binding energies and widths and the pion-nucleus interaction, *ibid.* **62**, 025202 (2000).
- [12] H. Nagahiro, S. Hirenzaki, E. Oset, and A. Ramos,  $\eta'$ -Nucleus optical potential and possible  $\eta'$  bound states, *Phys. Lett. B* **709**, 87 (2012).
- [13] M. Nanova *et al.*, Determination of the  $\eta'$ -nucleus optical potential, *Phys. Lett. B* **727**, 417 (2013).
- [14] M. Nanova *et al.*, Transparency ratio in  $\gamma A \rightarrow \eta' A'$  and the in-medium  $\eta'$  width, *Phys. Lett. B* **710**, 600 (2012).
- [15] E. Czerwiński *et al.*, Determination of the  $\eta'$ -Proton Scattering Length in Free Space, *Phys. Rev. Lett.* **113**, 062004 (2014).
- [16] H. Machner, Search for quasi bound  $\eta$  mesons, *J. Phys. G* **42**, 043001 (2015).
- [17] Q. Haider and L.-C. Liu, Eta-mesic nuclei: Past, present, future, *Int. J. Mod. Phys. E* **24**, 1530009 (2015).
- [18] K. Itahashi *et al.*, Feasibility study of observing  $\eta'$  mesic nuclei with  $(p, d)$  reaction, *Prog. Theor. Phys.* **128**, 601 (2012).
- [19] B. Jurado, K.-H. Schmidt, and K.-H. Behr, Application of a secondary-electron transmission monitor for high-precision intensity measurements of relativistic heavy-ion beams, *Nucl. Instrum. Methods Phys. Res., Sect. A* **483**, 603 (2002).
- [20] H. Geissel *et al.*, The GSI projectile fragment separator (FRS): A versatile magnetic system for relativistic heavy ions, *Nucl. Instrum. Methods Phys. Res., Sect. B* **70**, 286 (1992).

- [21] N. Iwasa, H. Geissel, G. Münzenberg, C. Scheidenberger, Th. Schwab, and H. Wollnik, MOCADI, a universal Monte Carlo code for the transport of heavy ions through matter within ion-optical systems, *Nucl. Instrum. Methods Phys. Res., Sect. B* **126**, 284 (1997).
- [22] H. Nagahiro, D. Jido, H. Fujioka, K. Itahashi, and S. Hirenzaki, Formation of  $\eta'(958)$ -mesic nuclei by the  $(p, d)$  reaction, *Phys. Rev. C* **87**, 045201 (2013).
- [23] From Fig. 3 in V. Yu. Grishina, L. A. Kondratyuk, M. Büscher, J. Haidenbauer, C. Hanhart, and J. Speth,  $\eta$ - and  $\eta'$ -meson production in the reaction  $pn \rightarrow dM$  near threshold, *Phys. Lett. B* **475**, 9 (2000), one can read the boundaries in the total cross section of  $pn \rightarrow d\eta'$  for the c.m. energy region of interest. The resultant range is in agreement with a calculation by K. Nakayama (private communication, 2012).